Climate and Air Quality Impact of Using Ammonia as an Alternative Shipping Fuel

Anthony Y. H. Wong[1], Noelle E. Selin[2,3], Sebastian D. Eastham[4,5*], Christine Mounaïm-Rouselle[6], Yiqi Zhang[7], Florian Allroggen[5]

[1]Center for Global Change Science, Massachusetts Institute of Technology, Cambridge, MA, USA

[2]Institute of Data, System and Society, Massachusetts Institute of Technology, Cambridge, MA, USA

[3]Department of Earth, Atmospheric, and Planetary Sciences, Massachusetts Institute of Technology, Cambridge, MA, USA

[4]Joint Program on the Science and Policy of Global Change, Massachusetts Institute of Technology, Cambridge, MA, USA

[5]Laboratory for Aviation and the Environment, Department of Aeronautics and Astronautics, Massachusetts Institute of Technology, Cambridge, MA, USA

[6]Laboratoire PRISME, Université d'Orléans, Orléans, France

[7]Division of Environment and Sustainability, Hong Kong University of Science and Technology, Clear Water Bay, Hong Kong, China

[*]Now at Department of Aeronautics, Faculty of Engineering, South Kensington Campus, London, United Kingdom

E-mail: `ayhwong@mit.edu`

Abstract. As carbon-free fuel, ammonia has been proposed as an alternative fuel to facilitate maritime decarbonization. Deployment of ammonia-powered ships is proposed as soon as 2024. However, emissions of NO_x, NH_3 and N_2O resulting from ammonia combustion could cause impacts on air quality and climate. In this study, we assess whether and under what conditions switching to ammonia fuel might affect climate and air quality. We use a bottom–up approach combining ammonia engine experiment results and ship track data to estimate global tailpipe NO_x, NH_3 and N_2O emissions from ammonia-powered ships with two possible engine technologies (NH_3–H_2 vs pure NH_3 combustion) under three emission regulation scenarios (with corresponding assumptions in emission control technologies). We then use the GEOS–Chem High Performance global chemical transport model to simulate the air quality impacts of switching to ammonia-powered ships. We find that the tailpipe N_2O emissions from ammonia-powered ships have climate impacts equivalent to 5.8% of current shipping CO_2 emissions. Globally, switching to NH_3–H_2 engines avoids 33,100 (18900 to 47300, 95% confidence interval) mortalities annually, while the unburnt NH_3 emissions (82.0 Tg NH_3 yr^{-1}) from pure NH_3 engines could lead

to 595,100 additional mortalities annually under current legislation. Requiring NH_3 scrubbing within current Emission Control Areas leads to smaller improvements in public health outcomes (38,000 avoided mortalities for NH_3–H_2 and 554,200 additional mortalities for pure NH_3 annually, respectively), while extending both Tier III NO_x standard and NH_3 scrubbing requirements globally leads to larger improvement in public health outcomes associated with a switch to ammonia-powered ships (79,100 and 21,100 avoided mortalities for NH_3–H_2 and pure NH_3 annually, respectively). Our findings suggest that while switching to ammonia fuel would reduce tailpipe greenhouse gas emissions from shipping, stringent ammonia emission control is required to mitigate the potential adverse effects on air quality.

1. Introduction

Maritime shipping burns heavy fuel oil in large diesel engines for energy (propulsion, heat, and electricity), which leads to emissions of CO_2 and air pollutants. The main air pollutants emitted by the maritime transport sector include SO_x (= SO_2+SO_4^{2-}), NO_x (= NO+NO_2), non-methane volatile organic compound (NMVOC), CO and carbonaceous aerosols. These are either components or precursors of particulate matter (PM) and ozone (O_3). Exposure to PM, particularly the fine PM (aerodynamic diameter < 2.5 μm, named $PM_{2.5}$) that can reach deep inside the respiratory tract, is estimated to have caused $3.7 - 4.8$ million deaths in 2015 by increasing the risk of cardiopulmonary and cerebrovascular diseases [6]. O_3 exposure exerts oxidative stress on the respiratory tract [27], which also leads to increased risk of cardiopulmonary diseases, and therefore another $1.04 - 1.24$ millions of respiratory deaths in 2010 globally [23]. Shipping emissions are estimated to account for 2.7% of global energy-related CO_2 emissions and caused an estimated $84800 - 103000$ annual premature deaths from $PM_{2.5}$ exposure globally in 2015 [41].

The International Maritime Organization (IMO) has outlined a goal of reducing greenhouse gas (GHG) emissions from international shipping by at least 40% by 2030 compared to the 2008 level [15]. The uses of alternative fuels (e.g. NH_3, H_2, methanol) and other energy solutions (e.g. electrification) are essential for reaching such a decarbonization goal [2]. NH_3 is one of the main candidates for alternative maritime fuels , and could represent up to 43% of the energy mix of shipping in 2050 [18]. Since NH_3 in mainly manufactured with H_2 and N_2 through Haber-Bosch Process, the carbon footprint of NH_3 production can be reduced by carbon capture (blue NH_3), or using renewable energy for N_2 and H_2 production and the synthesis process (green NH_3) [32].

Wolfram et al (2022) [37] summarized scientific concerns about the potential environmental impacts of using NH_3 as a marine fuel. NH_3 combustion may generate additional NO_x and N_2O compared to other fuels [12]. NH_3 emission is one of the major source of global $PM_{2.5}$ pollution [10] by neutralizing H_2SO_4 and HNO_3 in the

[81] atmosphere [19]. NH_3 emission leads to much higher $PM_{2.5}$ mortality costs per ton
[82] (\$23000 – 66000) than SO_2 (\$14000 – 24000) and NO_x (\$3800 – 14000) in the United
[83] States [11]. These show the potential danger of uncontrolled NH_3 emission via worsening
[84] $PM_{2.5}$ air quality. Emitted NO_x and NH_3 would then deposit to Earth's surface, causing
[85] damages to ecosystems (e.g. soil acidification and eutrophication) [28] and may lead to
[86] additional emission of N_2O [37], which is a potent greenhouse gas and contributes to
[87] stratospheric ozone depletion.

[88] Here, we explore the possible ranges of air quality and climate impacts of
[89] transitioning from using fossil fuels to ammonia as the major shipping fuel under
[90] different technologies and policies, aiming to highlight the opportunities and challenges
[91] of ammonia combustion as a strategy to decarbonize maritime transport.

2. Method

[93] We use a bottom–up approach to estimate the global NO_x, NH_3 and N_2O emissions
[94] from NH_3–powered ships as a function of engine technologies, emission control strategies
[95] and policy under 6 scenarios, using result from ammonia engine experiments and ship
[96] Automatic Identification System (AIS) data. We then simulate the associated changes
[97] in O_3 and $PM_{2.5}$ air quality using a global 3-D chemical transport model (GEOS-Chem
[98] High Performance). Finally, we estimate the impacts of simulated changes in O_3 and
[99] $PM_{2.5}$ on public health (expressed in annual premature mortalities) using concentration
[100] functions derived from epidemiological studies.

2.1. Scenarios

[102] In all scenarios, we apply an AIS-based shipping emission model [42] to estimate the
[103] global spatially-resolved pollutant and GHG emissions for every ship track in 2015
[104] following the technology and policy assumptions of each scenario. The emission model
[105] calculates ship emissions as a function of engine power demand, ship specifications,
[106] emission factors (EF) and activity time. Missing entries in ship specifications are filled
[107] based on the lengths and capacities of the associated ships. We choose the emission
[108] scenario with 0.5% cap on fuel sulphur content from Zhang et al (2021) [41] as our
[109] baseline. The "post–2020 NO_x baseline" scenario imposes the most stringent IMO NO_x
[110] emissions (Tier III) limit on top of baseline scenario, which represents the emissions
[111] from fossil fuel powered ships if all of them were retrofitted to follow IMO emission
[112] standards for newly–built ships.

[113] We consider the emissions from ammonia-powered ships with two types of engine
[114] technologies. The first type ("NH_3-H_2") is proposed by Imhoff et al (2021) [14]
[115] based on the experimental data from Lhuillier et al (2020) [22]. Part of the NH_3 is
[116] transferred to a catalytic NH_3 cracker to generate H_2 as the pilot fuel, which improves
[117] the stability of NH_3 ignition and combustion. This leads to less unburnt NH_3, but more
[118] NO_x emissions compared to pure NH_3 combustion. By balancing the NH_3 and NO_x

Table 1. Description of the engine technology and policy scenarios considered in this study. SCR refers to Selective Catalytic Reduction (assumed to be 90% effective), which converts NO_x and NH_3 into N_2 in 1:1 ratio under ideal conditions. NH_3 scrubbing is assumed to remove 95% of NH_3 slip after SCR. "Baseline" and "Post-2020 NO_x baseline" are shipping emissions from previous work derived from the same AIS-based method as this work. [41]

Scenario	Emission control inside current ECA	Emission control outside current ECA	Equivalent policy scenario
Baseline	2015 shipping with 0.5% sulphur cap		
Post-2020 NO_x baseline	Baseline with Tier III NO_x standard imposed globally		
$[NH_3–H_2]_{2020}$	SCR	SCR	2020 NO_x limit
$[NH_3–H_2]_{NH_3\_ECA\_LIM}$	SCR+NH_3 scrubbing	SCR	Additional NH_3 limit in ECA
$[NH_3–H_2]_{GLOB\_LIM}$	SCR+NH_3 scrubbing	SCR+NH_3 scrubbing	Global NO_x and NH_3 limits
$[Pure\ NH_3]_{2020}$	SCR	None	2020 NO_x limit
$[Pure\ NH_3]_{NH_3\_ECA\_LIM}$	SCR+NH_3 scrubbing	None	Additional NH_3 limit in ECA
$[Pure\ NH_3]_{GLOB\_LIM}$	SCR+NH_3 scrubbing	SCR+NH_3 scrubbing	Global NO_x and NH_3 limits

concentration in engine exhaust, both NO_x and NH_3 emissions can be controlled by Selective Catalytic Reduction (SCR). The second type of engine technology considered is pure NH_3 combustion [26], which provides certain advantages over the NH_3–H_2 technology described above (e.g. simpler design and lower NO_x emissions (fig. 1)). The derivations of EF and load dependencies for the two types of engines, and a discussion about the uncertainty in engine technologies are given as Supplemental Information.

We acknowledge the uncertainty in ammonia engine designs. Our engine technology scenarios do not intent to realistically replicate how ammonia combustion would be implemented on ships. Rather, the two engine technologies considered in our study reflects two extremes of, and therefore provide bounding scenarios for NO_x and NH_3 emission management approaches: 1) with pure NH_3 engine having low NO_x (currently regulated) and very high NH_3 (currently unregulated) emissions, versus 2) NH_3–H_2 engine that strictly maintains the NO_x/NH_3 ratio to allow SCR to simultaneously control both pollutants.

We consider three policy scenarios. The first ("2020") follows the IMO regulations as of 2020. The untreated NO_x EF are 32.7 g/kWh for NH_3–H_2 and 7.08 g/kWh for pure NH_3 engines following the load corrections prescribed by IMO [17] (fig. 1). Current IMO guidelines [16] cap NO_x EF for new vessels at 7.7 – 14.4 g/kWh (Tier II limit) when operating outside the Emission Control Area (ECA, mostly includes North America and United States Caribbean Sea as of 2020, and additionally Baltic Sea and North Sea in 2021) and 2 – 3.4 g/kWh (Tier III limit) within ECA, depending on the engines' rated speed. Compliance with such a guideline would require SCR that can remove
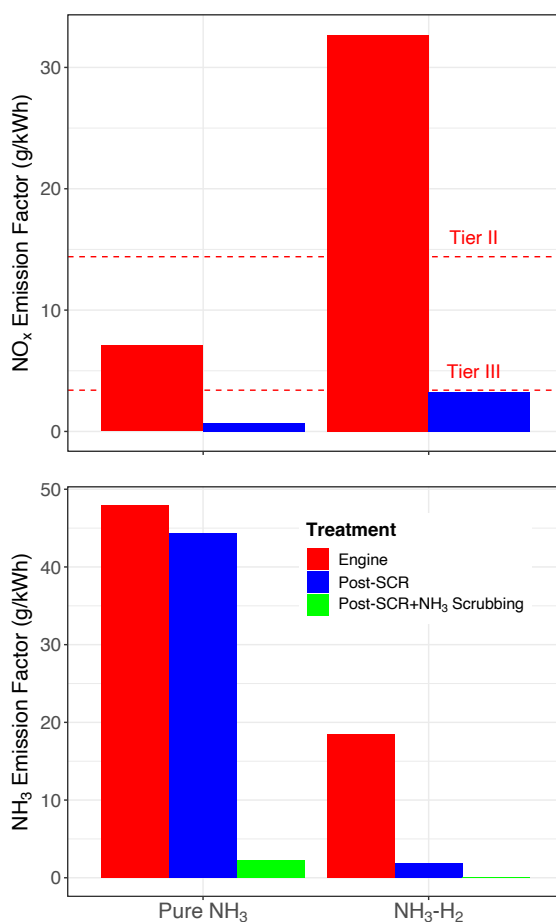
Figure 1. Load-corrected NH_3 and NO_x emission factors (EF) of pure NH_3 and NH_3–H_2 engines, as a function of emission control strategy. Red bar ("Engine") refers to EF from completely untreated engine exhaust. Blue (Post-SCR) and green bars (Post-SCR + NH_3 Scrubbing) refer to EF after implementations of emission control measures. SCR and NH_3 scrubbing are done sequentially. Red dotted lines indicate IMO NO_x regulations for slow engine speed (< 130 rpm), which is typical for large engine.

90% of NO_x to operate globally for NH_3–H_2 and within ECA only for pure NH_3 engines. The second ("NH_3_ECA_LIMIT") assumes that additional NH_3 scrubbing requirements (assumed to be 95% effective from available technology) [29, 33, 3] are implemented within ECA for both types of engines, while the third ("GLOB_LIM") extends Tier III NO_x compliance and NH_3 scrubbing requirements to the whole globe.

2.2. Atmospheric Chemistry Modeling

We use version 13.4.1 of the GEOS-Chem High Performance model (GCHP, https://doi.org/10.5281/zenodo.4429193) [24, 7] to simulate the response of O_3 and $PM_{2.5}$ to pollutant emission changes in each scenario through resolving the chemistry, transport, emission and deposition of relevant chemical species. The model is driven

by the Modern-Era Retrospective analysis for Research and Application (MERRA-2) assimilated meteorological fields [9]. The model is run at a horizontal resolution of 200km in cubed-sphere configuration (C48) from 1st Oct 2018 to 31st Dec 2019, with the first 3 months of output discarded as spin-up. O_3 is simulated from a coupled O_3-NO_x-VOCs-CO-halogen-aerosols chemical mechanism [30]. Anthropogenic emissions are from Community Emission Data System [13] except the shipping sector. Biogenic VOCs, soil NO_x and sea salt aerosol emissions follow Weng et al (2020) [35] and dust emissions follow Meng et al (2021) [25]. Formation of secondary inorganic aerosols are simulated by the ISORROPIA II [8], which considers thermodynamic equilibrium of the NH_4^+-Na^+-SO_4^{2-}-NO_3^--Cl^--H_2O. $PM_{2.5}$ concentrations are derived by summing the mass of its constituents at standard conditions to align with the sampling standard used by the United States Environmental Protection Agency [21]. Ship plume chemistry is parameterized by the PARANOX scheme [34], and the uncertainties in ammonia-powered ship plume is explored with additional simulations presented in Supplemental Information.

2.3. Health Outcome

We estimate the impacts of air quality changes on public health using the global gridded population density data at 30 arc-second resolution from the Gridded Population of the World version 4.11 [5]. O_3 and $PM_{2.5}$ concentrations are taken as the area-weighted averages from simulation grid cells overlapping with the 30 arc-second cell without any interpolation. Country-level age distribution and baseline mortality rates are provided by the World Health Organization (WHO) [36]. We estimate the risk of relative mortality from chronic O_3 and $PM_{2.5}$ exposure under the baseline (RR_{base}) and each alternative scenario i (RR_i) for every age group. The change in the annual mortality for scenario i ($\Delta Mort_i$) due to some disease for that age group is then calculated for each grid cell as:

$$\Delta Mort_i = Mort_{base}\frac{RR_i - RR_{base}}{RR_{base}} \tag{1}$$

where $Mort_{base}$ is the number of mortalities due to that disease in 2016. The relative risk is calculated by comparing the simulated exposure-relevant concentration under scenario i to that under the baseline scenario using an appropriate concentration response function (CRF). We use a log-linear CRF for O_3 that estimate a 12% increase (95% confidence interval (CI): $8.0 - 16\%$) in respiratory mortality per 10 ppb increase in annual mean maximum daily 8-hour average (MDA8) O_3 concentration [31]. For $PM_{2.5}$ we estimate RR for non-communicable diseases and lower respiratory infections using the age-specific non-linear CRFs from the Global Exposure Mortality Model [4].

We estimate the median and 95% confidence interval of changes in mortalities due to O_3 and $PM_{2.5}$ for each scenario by performing 1,000 random draws of the CRF parameters in a paired Monte-Carlo simulation.

Table 2. Modelled global total nitrogen-based air pollutants (in Tg/yr) and GHG emissions (in Tg $CO_{2,e}$/yr) from different scenarios. $CO_{2,e}$ (equivalent amount of CO_2 in terms of 100-year Global Warming Potential) is calculated as CO_2 emissions + (N_2O emissions $\times$ 273).

Scenario	NO_x (Tg/yr)	NH_3 (Tg/yr)	$CO_{2,e}$ (Tg/yr)
Baseline	17.2	0.004	867
Post-2020 NO_x baseline	3.59	0.004	867
$[NH_3-H_2]_{2020}$	4.43	2.51	50.2
$[NH_3-H_2]_{NH_3\_ECA\_LIM}$	4.43	2.21	50.2
$[NH_3-H_2]_{GLOB\_LIM}$	4.43	0.125	50.2
$[Pure\ NH_3]_{2020}$	6.84	82.0	50.2
$[Pure\ NH_3]_{NH_3\_ECA\_LIM}$	6.84	71.7	50.2
$[Pure\ NH_3]_{GLOB\_LIM}$	0.762	3.92	50.2
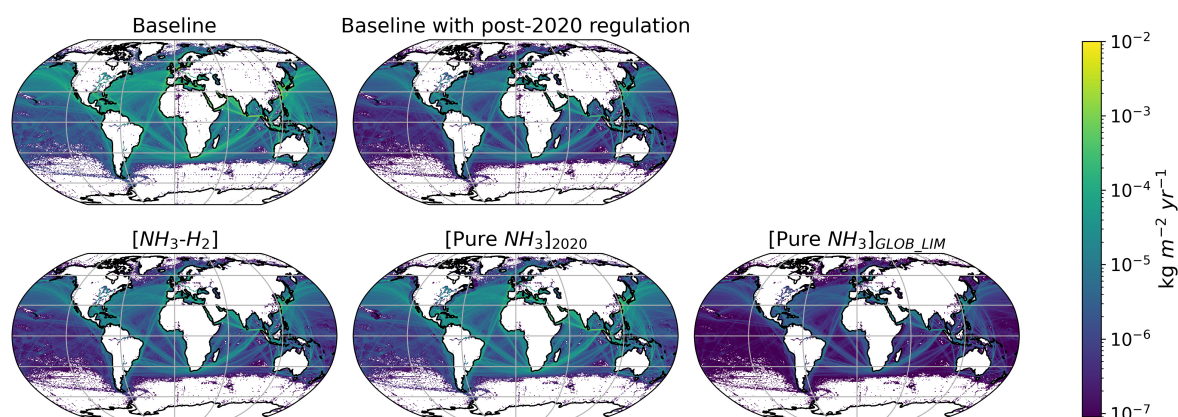
Figure 2. Spatial pattern of annual total NO_x emissions (kg m-2 yr^{-1}) under different scenarios.

3. Result

3.1. Modelled Shipping Emissions

Table 2 shows the modelled global annual shipping emissions of NO_x, NH_3 and GHG under different scenarios, and Figure 2 shows the spatial distribution of NO_x emissions. Under current regulations ("2020"), ammonia-powered ships have lower NO_x emissions (4.4 Tg NO_x/yr for NH_3–H_2 and 6.9 Tg NO_x/yr for pure NH_3). Such comparison mostly reflects regulatory rather than technological differences, since the older ships in the baseline scenario do not follow the newer and more stringent (Tier II or Tier III) NO_x regulations, while all newly built ammonia-powered ships abide the Tier II regulation outside ECA and Tier III regulations within ECA. To comply with Tier II NO_x regulations, SCR is required for the NH_3–H_2 engine while no NO_x control is needed for the pure NH_3 engine. This leads to higher total post-treatment NO_x emissions from pure NH_3 engines than that from NH_3–H_2 engines, despite pure NH_3 engines has lower
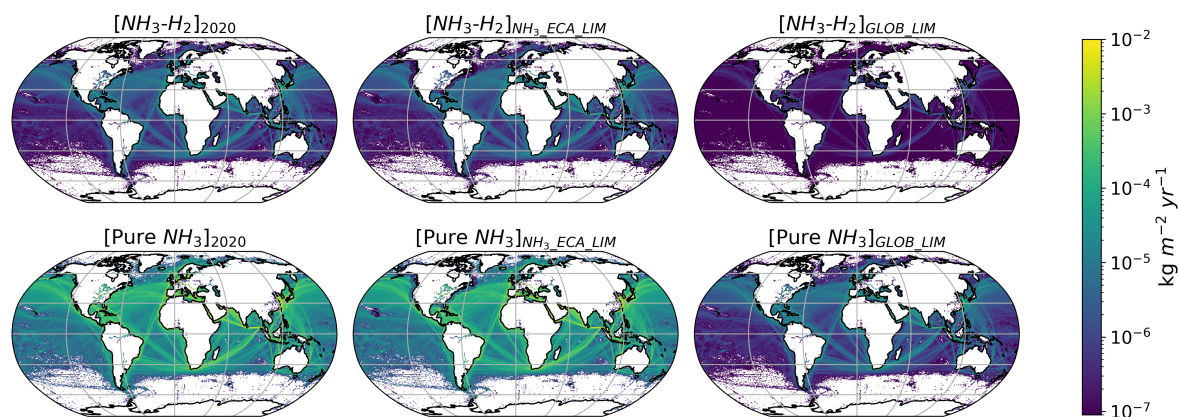
Figure 3. Spatial pattern of annual total NH_3 emissions (kg m-2 yr-1) under different scenarios.

pre-treatment NO_x emissions than NH_3–H_2 engines. If the Tier III NO_x regulations is enforced globally ("GLOB_LIM"), the NO_x emission of fossil fuel (3.6 Tg NO_x/yr) and NH_3–H_2 (4.4 Tg NO_x/yr) engines are similar, while pure NH_3 engines (0.8 Tg NO_x/yr) produce the lowest NO_x emissions.

Figure 3 shows the spatial distribution of modelled NH_3 emissions under different technology and policy scenarios. Under current regulations ("2020"), switching to NH_3-H_2 engines leads to 2.5 Tg/yr NH_3 emissions, while switching to pure NH_3 engines leads to NH_3 emissions (82.0 Tg/yr) that are 32.8 times higher than that from NH_3-H_2 engines. For pure NH_3 engines, SCR can only remove 7% of NH_3 from engine exhaust, leading to high tailpipe NH_3 emissions. In the "NH_3_ECA_LIM" scenario, which requires NH_3 scrubbing over ECA (mostly North American coast and northern Europe), global NH_3 emissions reduce by 12% for both NH_3-H_2 (2.2 Tg/yr) and pure NH_3 (71.7 Tg/yr) engines. In the "GLOB_LIM" scenario, with both SCR and NH_3 scrubbing are required globally, NH_3 emissions fall to 0.1 Tg/yr for NH_3–H_2 engines and 3.9 Tg/yr for pure NH_3 engines.

Table 2 also shows the long-lived GHG emissions from each scenario, given as the equivalent amount of CO_2 ($CO_{2,e}$) in terms of 100-year Global Warming Potential (GWP100) using a conversion factor of 273 from N_2O emission to $CO_{2,e}$ (Smith et al 2021). $CO_{2,e}$ from the baseline scenario does not include GHG other than CO_2 (mainly CH_4 and N_2O), which contribute to less than 3% of global shipping $CO_{2,e}$ during 2013 – 2015 (Olmer et al 2017). We find that the tailpipe $CO_{2,e}$ from the ammonia-powered fleet is 5.8% of that from the current fossil-fuel-powered fleet. Our analysis (see Supplemental Information) also shows that the "secondary N_2O emissions" from reactive nitrogen deposition (Wolfram et al 2022) is not a problem for NH_3-H_2 engine as the total reactive nitrogen emissions are lower than current fleets. For pure NH_3 engine, the net climate effects from nitrogen deposition are likely to be smaller than reduction in tailpipe GHG emissions (817.2 Tg $CO_{2,e}$/yr) from switching to ammonia-powered ships, showing the potential of blue and green ammonia as a climate-friendly shipping
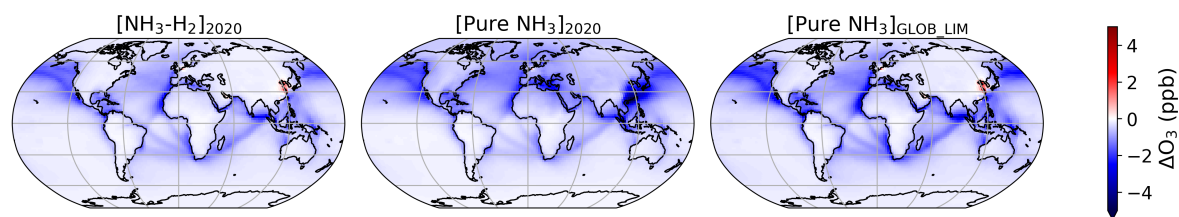
Figure 4. Changes in annual mean MDA8 O_3 concentration (ΔO_3, ppb) for different ammonia-powered ship scenarios

fuel, though considerable uncertainties exist on how CO_2 uptake and N_2O emissions respond to nitrogen deposition. This analysis, however, does not fully consider the life cycle GHG emissions (e.g. energy, methane slip) of NH_3 production.

3.2. Impacts on Air Quality

Figure 4 shows the modelled global changes in annual mean MDA8 O_3 due to converting current fleet to ammonia-powered ships with different technology and policy options. Generally, the lower NO_x emissions from ammonia-powered ships reduce annual mean MDA8 O_3. Under all scenarios, global population-weighted average MDA8 O_3 decreases (-0.27 ppb for $[NH_3\text{-}H_2]_{2020}$, -1.13 ppb for $[\text{Pure } NH_3]_{2020}$, -0.37 ppbv for $[\text{Pure } NH_3]_{\text{GLOB\_LIM}}$). The greatest reductions in population-weighted O_3 are simulated over coastal and island nations (e.g. 1.5 to 1.9 ppb for Sri Lanka and Djibouti, 1.4 to 2.2 ppb for Panama, 1.4 to 1.7 ppb for Jamaica). However, over highly NO_x–saturated coasts near northern China, northern Europe, and Persian Gulf, local increases in surface O_3 are simulated, especially under the scenarios with greater NO_x reductions ($[NH_3\text{-}H_2]_{2020}$ and $[\text{Pure } NH_3]_{\text{GLOB\_LIM}}$). Over North Sea, the NO_x–saturation leads to further increases in MDA8 O_3 as NO_x emissions become lower, increasing the population-weighted O_3 from 1 ppb under $[\text{Pure } NH_3]_{2020}$ to up to 1.5 ppb under $[\text{Pure } NH_3]_{\text{GLOB\_LIM}}$ over the Netherlands. Over East Asia, population-weighted MDA8 O_3 decreases by 2.4 ppb under the scenario with least NO_x reduction ($[\text{Pure } NH_3]_{2020}$), but increases by 0.2 ppb under $[\text{Pure } NH_3]_{\text{GLOB\_LIM}}$ and $[NH_3\text{-}H_2]_{2020}$ as NO_x emissions become lower. This shows the importance of local chemical environment in controlling the response of O_3 pollution to marine NO_x control.

In addition, we find substantial sensitivity of O_3 response to assumptions in ship plume chemistry (mainly NO_x lifetime, see Supplemental Material), which could be a major source of uncertainties. This shows the importance of understanding the plume chemistry of NH_3 ship in capturing the O_3 response.

Figure 5 shows the modelled changes in annual mean surface $PM_{2.5}$. Under $[NH_3\text{-}H_2]_{2020}$, population-weighted $PM_{2.5}$ increases by 0.21 μg m-3 (0.4%) over East Asia (definition of regions follows Giorgi et al (2001)). Smaller increases are simulated over western North America (0.08 μg m^{-3}), though the percentage increase (1.7%) is higher since the baseline population-weighted $PM_{2.5}$ (4.82 μg m^{-3}) is low. $PM_{2.5}$
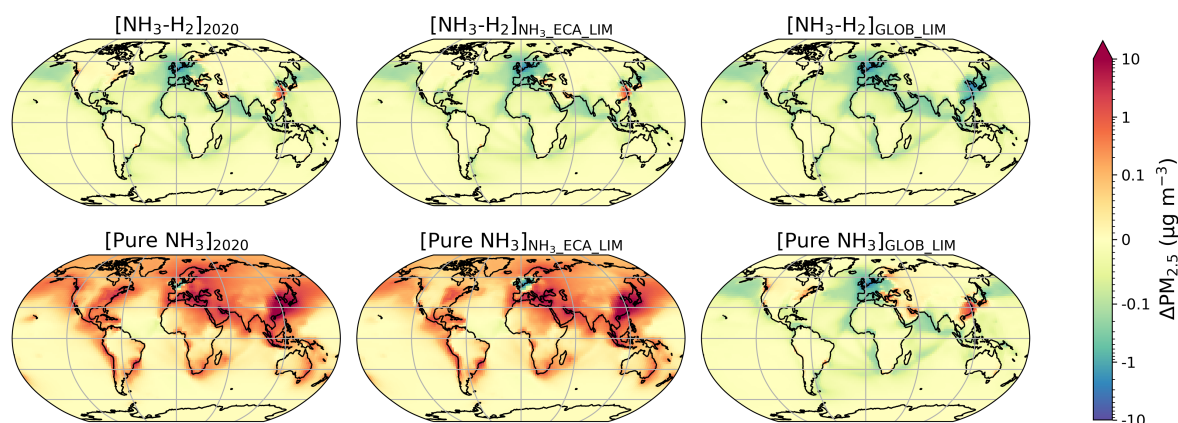
Figure 5. Changes in annual mean PM$_{2.5}$ concentration (ΔPM$_{2.5}$, μg m-3) for all ammonia-powered ships scenarios.

levels are mostly reduced over other regions in the world, especially over northern Europe and Mediterranean Basin, where population-weighted PM$_{2.5}$ decreases by 0.70 (4%) and 0.16 (0.6%) μg m^{-3}, respectively. Under [NH$_3$-H$_2$]$_{\text{NH}_3\_\text{ECA}\_\text{LIM}}$, population-weighted PM$_{2.5}$ is reduced by 0.82 μg m^{-3} (4.8%) and 0.055 μg m^{-3} (0.7%) over northern Europe and the United States, respectively, as NH$_3$ emission control is enforced over those regions. Under [NH$_3$-H$_2$]$_{\text{GLOB}\_\text{LIM}}$, both Tier III NO$_x$ and NH$_3$ emission limit are extended globally, resulting in reduced PM$_{2.5}$ levels over the whole globe. Particularly, the negative impacts from NH$_3$ emission over Mediterranean Basin and East Asia are successfully mitigated, resulting in 0.33 (1.4%) and 0.62 μg m^{-3} (1.2%) of reduction in population-weighted PM$_{2.5}$, respectively.

Pure NH$_3$ engines have high NH$_3$ emission, leading to higher PM$_{2.5}$ levels than NH$_3$-H$_2$ engines under the same policy scenarios. Under [Pure NH$_3$]$_{2020}$, PM$_{2.5}$ increases globally expect over the North Sea. Reduction in NO$_x$ emissions lead to lower population-weighted PM$_{2.5}$ over Netherlands (1.86 μg m^{-3}, 9.0%), Denmark (0.50 μg m^{-3}, 3.2%), and Belgium (0.35 μg m^{-3}, 2.0%). The largest increases in population-weighted PM$_{2.5}$ are simulated over East Asia (11.4 μg m^{-3}, 21.2%), North Africa (3.40 μg m^{-3}, 5.5%), Mediterranean Basin (3.36 μg m^{-3}, 14.6%), Southeast Asia (2.7 μg m^{-3}, 14.2%), western North America (1.20 μg m^{-3}, 24.8%) and eastern North America (1.88 μg m^{-3}, 21.7%). Under [Pure NH$_3$]$_{\text{NH}_3\_\text{ECA}\_\text{LIM}}$, the increase of PM$_{2.5}$ over northern Europe (0.058 μg m^{-3}, 0.34% vs 0.74 μg m^{-3}, 4.3% under [Pure NH$_3$]$_{2020}$), eastern North America (0.35 μg m^{-3}, 7.2%) and western North America (0.55 μg m^{-3}, 6.3%) are partially mitigated by the NH$_3$ emission control. When NH$_3$ emission control is required globally ([Pure NH$_3$]$_{\text{GLOB}\_\text{LIM}}$), the spatial pattern of PM$_{2.5}$ changes largely resembles that from [NH$_3$-H$_2$]$_{2020}$ due to comparable combined NO$_x$+NH$_3$ emissions (4.7 Tg/yr for [Pure NH$_3$]$_{\text{GLOB}\_\text{LIM}}$ vs 6.9 Tg/yr for [NH$_3$-H$_2$]$_{2020}$). Despite having lower combined NO$_x$+NH$_3$ emissions, [Pure NH$_3$]$_{\text{GLOB}\_\text{LIM}}$ has higher PM$_{2.5}$ levels than [NH$_3$-H$_2$]$_{2020}$ due to higher NH$_3$ emissions (3.9 Tg/yr for [Pure NH$_3$]$_{\text{GLOB}\_\text{LIM}}$ vs 2.5 Tg/yr for [NH$_3$-H$_2$]$_{2020}$) globally except over northern Europe.

Table 3. Estimated changes in annual global mortality attributable to PM$_{2.5}$ ($\Delta M_{PM_{2.5}}$), O$_3$ (ΔM_{O_3}), and their sum (ΔM_{total}) from each scenario. Parentheses indicates 95% confidence interval (CI) of the estimates from 1000 Monte-Carlo simulations.

Scenario	$\Delta M_{PM_{2.5}}$	ΔM_{O_3}	ΔM_{total}
[NH$_3$–H$_2$]$_{2020}$	-16,900 (-24,000;-10,000)	-16,200 (-23,300;-9,000)	-33,100 (-47,300;-18,900)
[NH$_3$–H$_2$]$_{NH_3\_ECA\_LIM}$	-22,100 (-29,800;-8,700)	-15,900 (-23,000;-8,700)	-38,000 (-52,000;-23,100)
[NH$_3$–H$_2$]$_{GLOB\_LIM}$	-66,500 (-78,800;54,400)	-12,600 (19,900;-5,200)	-79,100 (-98,700;59,600)
[Pure NH$_3$]$_{2020}$	+668,100 (+542,600;+797,300)	-73,100 (-94,600;-51,100)	+595,100 (+448,000;+746,200)
[Pure NH$_3$]$_{NH_3\_ECA\_LIM}$	+623,900 (+504,000;+747,300)	-69,700 (-90,300;-48,700)	+554,200 (+413,700;+698,600)
[Pure NH$_3$]$_{GLOB\_LIM}$	+1,200 (-10,200;+12,700)	-22,400 (-31,600;-13,000)	-21,1000 (-41,800;-300)
Post-2020 NO$_x$ basline	-46,200 (-54,800;-37,700)	-13,000 (-21,100;-4,800)	-59,100 (-75,900;-42,500)

288 In addition, we find that NH$_3$ could potentially form PM$_{2.5}$ with anions and acids
289 in sea spray, which implies extra sensitivity of PM$_{2.5}$ to NH$_3$ emissions that could not be
290 controlled by reducing NO$_x$ and SO$_x$ emissions alone (see Supplemental Information).

291 *3.3. Health Impacts*

292 Table 3 shows the changes in annual global mortality attributable to O$_3$ (ΔM_{O_3}) and
293 PM$_{2.5}$ ($\Delta M_{PM_{2.5}}$) for each scenario. We estimate that current shipping emissions leads to
294 87,400 and 16,900 mortalities from PM$_{2.5}$ and O$_3$, respectively. The lower NO$_x$ emissions
295 from ammonia-powered ships provide significant O$_3$ air quality benefit, reducing annul
296 O$_3$-related mortality by 12,600 to 73,100. Despite the lack of primary PM (BC, OC) and
297 secondary PM precursors (SO$_2$, NMVOC) emissions other than NO$_x$ and NH$_3$, ammonia-
298 powered ships lead to worse $\Delta M_{PM_{2.5}}$ (-22,100 to +668,100) than fossil fuel powered ships
299 with similar NO$_x$ regulation ("Post-2020 NO$_x$ Baseline", -46,200) except the scenario
300 with lowest NH$_3$ emissions ([NH$_3$-H$_2$]$_{GLOB\_LIM}$), -66,500). This highlights the importance
301 of NH$_3$ as a PM$_{2.5}$ precursor in coastal environment, and therefore minimizing tailpipe
302 NH$_3$ emission to mitigate the negative air quality impacts from ammonia-powered ships.
303 Under currently legislation ("2020"), switching to NH$_3$–H$_2$ engine reduces annual
304 global mortalities by 33,100, attributable to both changes in PM$_{2.5}$ (51%) and O$_3$
305 (49%). While providing substantial benefits from reducing O$_3$–related mortality (-
306 73,100), switching to pure NH$_3$ engines increases in PM$_{2.5}$–related mortality (+668,100),
307 causing a net effect of 595,100 increased mortalities. This is mostly due to the increased
308 mortality over East Asia (+468,400; 79% of ΔM_{total}). Since current ECA are mostly over
309 North America and northern Europe, additional NH$_3$ emissions control over current ECA

("NH$_3$_ECA_LIM") only provides marginal benefits in terms of mortalities (4,900 (13%) for NH$_3$-H$_2$ engines and 40,900 (7%) for pure NH$_3$ engines) since most of the increases in PM$_{2.5}$ occur overs East Asia, North Africa, Southeast Asia and Mediterranean region. In contrast, when both Tier III NO$_x$ and NH$_3$ emission controls are extended globally ("GLOB_LIM"), the negative impacts of pure NH$_3$ engines on PM$_{2.5}$ can be largely mitigated, leading a net reduction in mortalities (-21,100). For NH$_3$–H$_2$ engines, the low NH$_3$ emissions, and therefore global reduction in PM$_{2.5}$ level, lead to substantial reduction in mortalities (-79,100) equivalent to 76% of mortalities attributable to current shipping emissions.

4. Discussion

Using blue and green NH$_3$ to facilitate decarbonization of maritime transport has been gaining traction among the industry, while concerns have been raised about the consequences (e.g. secondary N$_2$O emissions, air pollution, eutrophication, soil acidification) of such large additional reactive nitrogen production and emission into the Earth System [1, 37]. Despite the uncertainties in the engine design, fuel mix, emission factors and plume chemistry of ammonia-powered ships as they are not yet deployed in real world, an early evaluation using currently available information can provide information to help stakeholders identify the potential climate and air quality issues and formulate mitigation measures.

We combine results from engine experiments and ship activity data to estimate the possible GHG and air pollutant emissions and impacts from ammonia-powered ships. We find that the GWP attributable to tailpipe N$_2$O emissions from ammonia-powered fleet is a small fraction (5.8%) of that of the current fleet. Our findings confirm the potential of blue and green NH$_3$ as a climate-friendly shipping fuel. However, the impacts of large reactive nitrogen deposition over land ecosystems on GHG balance remain highly uncertain.

We find that the public health impacts of switching from fossil fuel to ammonia depends largely on the technology and policy choices. If tuned to balance NO$_x$ and NH$_3$ concentration from engine exhaust to allow simultaneous reduction of NO$_x$ and NH$_3$ emissions using well-optimized exhaust post-treatment systems with highly efficient combustion modes, deployment of ammonia combustion technology can lead to net health benefits by reducing both O$_3$ and PM$_{2.5}$ levels. If the engines are tuned to have lower NO$_x$ emissions than NH$_3$–H$_2$ combustion, which is more compatible with current NO$_x$–focused regulatory framework, the unburnt NH$_3$ emission, if unmitigated, can lead to large increases in PM$_{2.5}$, and consequently 595,100 additional global premature mortalities annually. Imposing NH$_3$ emission regulation over current ECA only mitigates 7% of the increases in annual mortalities from pure NH$_3$ engines, since the largest negative impacts are expected over East Asia, which is not currently part of any ECAs. Extending stringent control of NO$_x$ and NH$_3$ emissions to the globe provides substantial air quality benefits. This shows the urgency of updating shipping emission regulations

in anticipation of the real–world deployment of ammonia-powered-ships. Particularly, given the availability of effective ($> 95\%$) NH_3 removal strategies, priority should be given towards developing and enforcing working NH_3 emission regulations. Our additional simulations (see Supplemental Information) shows that these conclusions are not affected by the assumptions in plume chemistry, though better understanding plume chemistry of ammonia-powered ships could help better evaluate the O_3 impacts.

The practicality and efficacy of SCR for ammonia engines remain highly uncertain. The lack of sulfur and particulate poisoning of catalyst, and not requiring a separate NH_3 source to operate could potentially lead to cheaper SCR operation since catalyst and urea recharge are estimated to account for at least 61% of the total cost of SCR ownership and operation [40]. However, NH_3 combustion generates more H_2O than diesel combustions (see Supplemental Information), which limits the efficacy of SCR [20, 38]. Excessive tailpipe N_2O emissions can result from mistuned SCR and ammonia oxidation systems [39], which could potentially offset the climate benefits. Optimizing the SCR systems for ammonia engines is crucial to limiting their potential air quality and climate impacts.

Our study shows the feasibility of NH_3 to be a climate-friendly shipping fuel despite the concern on tailpipe N_2O emission, and highlights the adverse effects of unburnt NH_3 emissions on $PM_{2.5}$ air quality, which can be mitigated by emission control measures feasible under current technology. Minimizing tailpipe NO_x and NH_3 emission through engine design, emission control technologies and regulations is critical for ammonia-powered ships to provide positive impact on air quality and prevent negative impacts from excessive nitrogen deposition, alongside reducing GHG emissions. Further studies are required to understand other environmental impacts (e.g. NH_3 leakage, GHG emissions from NH_3 production) of using NH_3 as shipping fuel from a life-cycle perspective.

5. Acknowledgement

References

[1] Cornelia Baessler et al., eds. *Atlas of Ecosystem Services: Drivers, Risks, and Societal Responses*. 1st ed. 2019. Cham: Springer International Publishing : Imprint: Springer, 2019. 1 p. ISBN: 978-3-319-96229-0. DOI: 10.1007/978-3-319-96229-0.

[2] Paul Balcombe et al. "How to decarbonise international shipping: Options for fuels, technologies and policies". In: *Energy Conversion and Management* 182 (Feb. 2019), pp. 72–88. ISSN: 01968904. DOI: 10.1016/j.enconman.2018.12.080. URL: https://linkinghub.elsevier.com/retrieve/pii/S0196890418314250 (visited on 12/21/2023).

[3] Andrea Boero et al. "Environmental assessment of road transport fueled by ammonia from a life cycle perspective". In: *Journal of Cleaner Production* 390 (Mar. 2023), p. 136150. ISSN: 09596526. DOI: 10.1016/j.jclepro.2023.136150. URL: https://linkinghub.elsevier.com/retrieve/pii/S0959652623003086 (visited on 12/21/2023).

[4] Richard Burnett et al. "Global estimates of mortality associated with longterm exposure to outdoor fine particulate matter". In: *Proceedings of the National Academy of Sciences of the United States of America* 115.38 (Sept. 18, 2018). Publisher: National Academy of Sciences, pp. 9592–9597. ISSN: 10916490. DOI: 10.1073/pnas.1803222115.

[5] Center For International Earth Science Information Network-CIESIN-Columbia University. *Gridded Population of the World, Version 4 (GPWv4): National Identifier Grid, Revision 11.* 2018. DOI: 10.7927/H4TD9VDP. URL: https://sedac.ciesin.columbia.edu/data/set/gpw-v4-national-identifier-grid-rev11 (visited on 12/21/2023).

[6] Aaron J. Cohen et al. "Estimates and 25-year trends of the global burden of disease attributable to ambient air pollution: an analysis of data from the Global Burden of Diseases Study 2015". In: *The Lancet* 389.10082 (2017). ISBN: 0000030449, pp. 1907–1918. ISSN: 1474547X. DOI: 10.1016/S0140-6736(17)30505-6.

[7] Sebastian D. Eastham et al. "GEOS-Chem High Performance (GCHP v11-02c): a next-generation implementation of the GEOS-Chem chemical transport model for massively parallel applications". In: *Geoscientific Model Development* 11.7 (July 24, 2018), pp. 2941–2953. ISSN: 1991-9603. DOI: 10.5194/gmd-11-2941-2018. URL: https://gmd.copernicus.org/articles/11/2941/2018/ (visited on 12/21/2023).

[8] C. Fountoukis and A. Nenes. "ISORROPIAII: A computationally efficient thermodynamic equilibrium model for K+-Ca2+-Mg2+-NH4+-Na+-SO42–NO3–Cl–H2O aerosols". In: *Atmospheric Chemistry and Physics* 7.17 (2007). ISBN: 1680-7316, pp. 4639–4659. ISSN: 1680-7324. DOI: 10.5194/acp-7-4639-2007.

[9] Ronald Gelaro et al. "The modern-era retrospective analysis for research and applications, version 2 (MERRA-2)". In: *Journal of Climate* 30.14 (2017), pp. 5419–5454. ISSN: 08948755. DOI: 10.1175/JCLI-D-16-0758.1.

[10] Baojing Gu et al. "Abating ammonia is more cost-effective than nitrogen oxides for mitigating PM $_{2.5}$ air pollution". In: *Science* 374.6568 (Nov. 5, 2021), pp. 758–762. ISSN: 0036-8075, 1095-9203. DOI: 10.1126/science.abf8623. URL: https://www.science.org/doi/10.1126/science.abf8623 (visited on 12/21/2023).

[11] Jinhyok Heo, Peter J. Adams, and H. Oliver Gao. "Public Health Costs of Primary PM $_{2.5}$ and Inorganic PM $_{2.5}$ Precursor Emissions in the United States". In: *Environmental Science & Technology* 50.11 (June 7, 2016), pp. 6061–6070. ISSN: 0013-936X, 1520-5851. DOI: 10.1021/acs.est.5b06125. URL: https://pubs.acs.org/doi/10.1021/acs.est.5b06125 (visited on 12/21/2023).

[12] Satoshi Hinokuma and Kazuhiko Sato. "Ammonia Combustion Catalysts". In: *Chemistry Letters* 50.4 (Apr. 5, 2021), pp. 752–759. ISSN: 0366-7022, 1348-0715. DOI: 10.1246/cl.200843. URL: http://www.journal.csj.jp/doi/10.1246/cl.200843 (visited on 12/21/2023).

[13] Rachel M. Hoesly et al. "Historical (1750–2014) anthropogenic emissions of reactive gases and aerosols from the Community Emissions Data System (CEDS)". In: *Geoscientific Model Development* 11.1 (Jan. 29, 2018), pp. 369–408. ISSN: 1991-9603. DOI: 10.5194/gmd-11-369-2018. URL: https://gmd.copernicus.org/articles/11/369/2018/ (visited on 12/21/2023).

[14] Thomas Buckley Imhoff, Savvas Gkantonas, and Epaminondas Mastorakos. "Analysing the Performance of Ammonia Powertrains in the Marine Environment". In: *Energies* 14.21 (Nov. 8, 2021), p. 7447. ISSN: 1996-1073. DOI: 10.3390/en14217447. URL: https://www.mdpi.com/1996-1073/14/21/7447 (visited on 12/21/2023).

[15] International Maritime Organization. *INITIAL IMO STRATEGY ON RE-DUCTION OF GHG EMISSIONS FROM SHIPS Contents*. 2018. (Visited on 03/23/2023).

[16] International Maritime Organization. *Nitrogen Oxides (NOx) – Regulation 13*. 2017. URL: https://www.imo.org/en/OurWork/Environment/Pages/Nitrogen-oxides-(NOx)-%E2%80%93-Regulation-13.aspx (visited on 11/06/2023).

[17] International Maritime Organization. *Technical Code on Control of Emission of Nitrogen Oxides from Marine Diesel Engines*. 2008.

[18] IRENA. *A pathway to decarbonise the shipping sector by 2050*. International Renewable Energy Agency, 2021. ISBN: 978-92-9260-330-4.

[19] Daniel J. Jacob. *Introduction to Atmospheric Chemistry*. Princeton University Press, 1999. 267 pp.

[20] Kacper Kuta et al. "Experimental and numerical investigation of dual-fuel CI ammonia engine emissions and after-treatment with V2O5/SiO2–TiO2 SCR". In: *Fuel* 334 (Feb. 2023), p. 126523. ISSN: 00162361. DOI: 10.1016/j.fuel.2022.126523. URL: https://linkinghub.elsevier.com/retrieve/pii/S0016236122033476 (visited on 01/29/2024).

[21] Robyn N. C. Latimer and Randall V. Martin. "Interpretation of measured aerosol mass scattering efficiency over North America using a chemical transport model". In: *Atmospheric Chemistry and Physics* 19.4 (Feb. 28, 2019), pp. 2635–2653. ISSN: 1680-7324. DOI: 10.5194/acp-19-2635-2019. URL: https://acp.copernicus.org/articles/19/2635/2019/ (visited on 12/21/2023).

[22] Charles Lhuillier et al. "Experimental study on ammonia/hydrogen/air combustion in spark ignition engine conditions". In: *Fuel* 269 (June 2020), p. 117448. ISSN: 00162361. DOI: `10.1016/j.fuel.2020.117448`. URL: `https://linkinghub.elsevier.com/retrieve/pii/S0016236120304439` (visited on 12/21/2023).

[23] Christopher S. Malley et al. "Updated Global Estimates of Respiratory Mortality in Adults 30Years of Age Attributable to Long-Term Ozone Exposure". In: *Environmental Health Perspectives* 125.8 (Aug. 16, 2017), p. 087021. ISSN: 0091-6765, 1552-9924. DOI: `10.1289/EHP1390`. URL: `https://ehp.niehs.nih.gov/doi/10.1289/EHP1390` (visited on 11/28/2023).

[24] Randall V. Martin et al. "Improved advection, resolution, performance, and community access in the new generation (version 13) of the high-performance GEOS-Chem global atmospheric chemistry model (GCHP)". In: *Geoscientific Model Development* 15.23 (Dec. 1, 2022), pp. 8731–8748. ISSN: 1991-9603. DOI: `10.5194/gmd-15-8731-2022`. URL: `https://gmd.copernicus.org/articles/15/8731/2022/` (visited on 12/21/2023).

[25] Jun Meng et al. "Grid-independent high-resolution dust emissions (v1.0) for chemical transport models: application to GEOS-Chem (12.5.0)". In: *Geoscientific Model Development* 14.7 (July 6, 2021), pp. 4249–4260. ISSN: 1991-9603. DOI: `10.5194/gmd-14-4249-2021`. URL: `https://gmd.copernicus.org/articles/14/4249/2021/` (visited on 12/21/2023).

[26] Christine Mounaïm-Rousselle et al. "Performance of ammonia fuel in a spark assisted compression Ignition engine". In: *International Journal of Engine Research* 23.5 (May 2022), pp. 781–792. ISSN: 1468-0874, 2041-3149. DOI: `10.1177/14680874211038726`. URL: `http://journals.sagepub.com/doi/10.1177/14680874211038726` (visited on 12/21/2023).

[27] Daniela Nuvolone, Davide Petri, and Fabio Voller. "The effects of ozone on human health". In: *Environmental Science and Pollution Research* 25.9 (Mar. 2018), pp. 8074–8088. ISSN: 0944-1344, 1614-7499. DOI: `10.1007/s11356-017-9239-3`. URL: `http://link.springer.com/10.1007/s11356-017-9239-3` (visited on 12/21/2023).

[28] Richard J. Payne et al. "Nitrogen deposition and plant biodiversity: past, present, and future". In: *Frontiers in Ecology and the Environment* 15.8 (2017), pp. 431–436. ISSN: 15409309. DOI: `10.1002/fee.1528`.

[29] R. W. Melse and N. W. M. Ogink. "Air scrubbing techniques for ammonia and odor reduction at livestock operations: Review of on-farm research in the Netherlands". In: *Transactions of the ASAE* 48.6 (2005), pp. 2303–2313. ISSN: 2151-0059. DOI: `10.13031/2013.20094`. URL: `http://elibrary.asabe.org/abstract.asp??JID=3&AID=20094&CID=t2005&v=48&i=6&T=1` (visited on 12/21/2023).

[30] Tomás Sherwen et al. "Global impacts of tropospheric halogens (Cl, Br, I) on oxidants and composition in GEOS-Chem". In: *Atmospheric Chemistry and Physics* 16.18 (Sept. 29, 2016), pp. 12239–12271. ISSN: 1680-7324. DOI: `10.5194/acp-16-12239-2016`. URL: `https://acp.copernicus.org/articles/16/12239/2016/` (visited on 12/21/2023).

[31] Michelle C. Turner et al. "Long-Term Ozone Exposure and Mortality in a Large Prospective Study". In: *American Journal of Respiratory and Critical Care Medicine* 193.10 (May 15, 2016), pp. 1134–1142. ISSN: 1073-449X, 1535-4970. DOI: `10.1164/rccm.201508-1633OC`. URL: `https://www.atsjournals.org/doi/10.1164/rccm.201508-1633OC` (visited on 12/21/2023).

[32] A. Valera-Medina et al. "Review on Ammonia as a Potential Fuel: From Synthesis to Economics". In: *Energy & Fuels* 35.9 (May 6, 2021), pp. 6964–7029. ISSN: 0887-0624, 1520-5029. DOI: `10.1021/acs.energyfuels.0c03685`. URL: `https://pubs.acs.org/doi/10.1021/acs.energyfuels.0c03685` (visited on 01/29/2024).

[33] Caroline Van Der Heyden, Peter Demeyer, and Eveline I.P. Volcke. "Mitigating emissions from pig and poultry housing facilities through air scrubbers and biofilters: State-of-the-art and perspectives". In: *Biosystems Engineering* 134 (June 2015), pp. 74–93. ISSN: 15375110. DOI: `10.1016/j.biosystemseng.2015.04.002`. URL: `https://linkinghub.elsevier.com/retrieve/pii/S1537511015000653` (visited on 12/21/2023).

[34] G. C. M. Vinken et al. "Accounting for non-linear chemistry of ship plumes in the GEOS-Chem global chemistry transport model". In: *Atmospheric Chemistry and Physics* 11.22 (Nov. 23, 2011), pp. 11707–11722. ISSN: 1680-7324. DOI: `10.5194/acp-11-11707-2011`. URL: `https://acp.copernicus.org/articles/11/11707/2011/` (visited on 12/21/2023).

[35] Hongjian Weng et al. "Global high-resolution emissions of soil NOx, sea salt aerosols, and biogenic volatile organic compounds". In: *Scientific Data* 7.1 (May 20, 2020), p. 148. ISSN: 2052-4463. DOI: `10.1038/s41597-020-0488-5`. URL: `https://www.nature.com/articles/s41597-020-0488-5` (visited on 12/21/2023).

[36] WHO. *WHO methods and data sources for country-level causes of death 2000-2016*. 2018. URL: `https://terrance.who.int/mediacentre/data/ghe/healthinfo/Deaths/GHE2016_COD_methods.pdf`.

[37] Paul Wolfram et al. "Using ammonia as a shipping fuel could disturb the nitrogen cycle". In: *Nature Energy* 7.12 (Dec. 1, 2022). Publisher: Nature Research, pp. 1112–1114. ISSN: 20587546. DOI: `10.1038/s41560-022-01124-4`.

[38] Pan Xiang et al. "Experimental investigation on gas emission characteristics of ammonia/diesel dual-fuel engine equipped with DOC + SCR aftertreatment". In: *Fuel* 359 (Mar. 2024), p. 130496. ISSN: 00162361. DOI: `10.1016/j.fuel.2023.130496`. URL: `https://linkinghub.elsevier.com/retrieve/pii/S0016236123031101` (visited on 01/29/2024).

[39] Malcolm Yates et al. "N2O formation in the ammonia oxidation and in the SCR process with V2O5-WO3 catalysts". In: *Catalysis Today* 107-108 (Oct. 2005), pp. 120–125. ISSN: 09205861. DOI: `10.1016/j.cattod.2005.07.015`. URL: `https://linkinghub.elsevier.com/retrieve/pii/S0920586105004086` (visited on 12/21/2023).

[40] Guangwei Zhang et al. "Relation analysis on emission control and economic cost of SCR system for marine diesels". In: *Science of The Total Environment* 788 (Sept. 2021), p. 147856. ISSN: 00489697. DOI: `10.1016/j.scitotenv.2021.147856`. URL: `https://linkinghub.elsevier.com/retrieve/pii/S0048969721029272` (visited on 12/21/2023).

[41] Yiqi Zhang et al. "Global air quality and health impacts of domestic and international shipping". In: *Environmental Research Letters* 16.8 (2021), p. 084055. ISSN: 17489326. DOI: `10.1088/1748-9326/ac146b`.

[42] Yiqi Zhang et al. "The significance of incorporating unidentified vessels into AIS-based ship emission inventory". In: *Atmospheric Environment* 203 (Apr. 2019), pp. 102–113. ISSN: 13522310. DOI: `10.1016/j.atmosenv.2018.12.055`. URL: `https://linkinghub.elsevier.com/retrieve/pii/S1352231019300226` (visited on 12/21/2023).

Supplemental Information

Additional details in deriving EF for the pure NH₃ and NH₃–H₂ engines
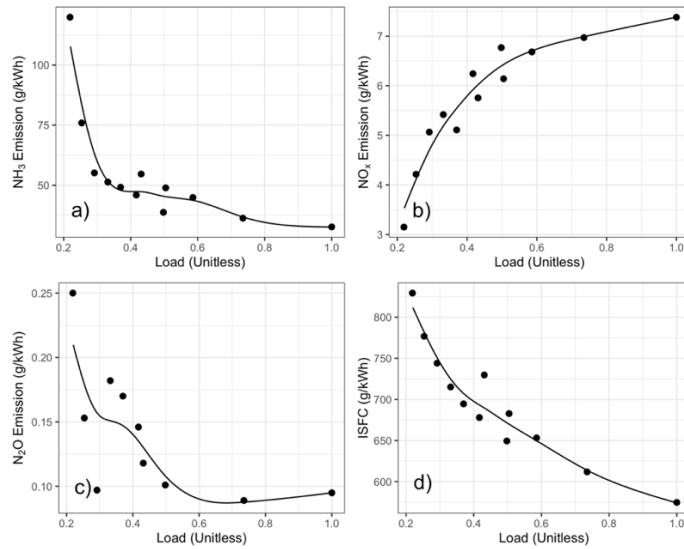
Fig. S1 Emission factors (a – c) and indicated specific fuel consumption (ISFC, d) as the function of engine load for pure NH₃ drivetrain. Dots indicate the raw data from (Mounaïm-Rousselle *et al* 2022), and lines indicate the generalized additive model fitting.

The engine EF for pure NH₃ engines follow the experiment result of Mounaïm-Rousselle *et al* (2022) corrected by the same drivetrain mechanical efficiency (92.5%) implied by Imhoff *et al* (2021), with a generalized additive model to derive the continuous load curves (Fig. S1a – 1c). We do not extrapolate the EF and ISFC beyond engine load < 20% due to the lack of data.

The engine EF of NH₃–H₂ is significantly more complicated due to the possibility of varying NH₃:H₂ ratio to achieve different efficiency, engine stability and emission profile (Mercier *et al* 2022, Lhuillier *et al* 2020). We assume the drivetrain EF before any treatment presented by Imhoff *et al* (2021) (29.4 g NOₓ/kWh and 16.7 g NH₃/kWh) are representative of the emissions at full engine load.
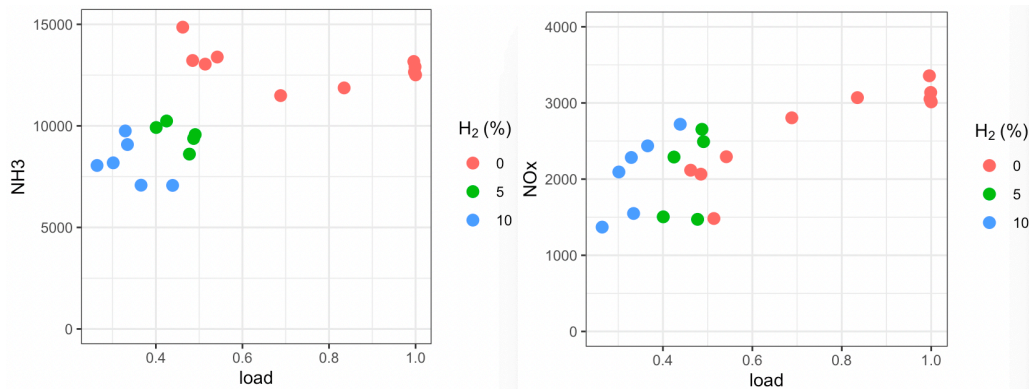
Fig. S2 Engine exhaust NH₃ and NOₓ concentration as a function of engine load and hydrogen fraction in the fuel mix from an NH₃–H₂ engine test (Mounaïm-Rousselle *et al* 2021)

The data from Mounaïm-Rousselle *et al* (2021) (Fig. S2) suggest that as engine load decreases and H_2 fraction is held constant, NH_3 EF increases while NO_x EF decreases. However, the introduction of additional H_2 as load decreases, which serves as the combustion promoter to improve engine stability and performance, partially offsetting the trends in NO_x and NH_3 EF.

We assume that the NH_3–H_2 engines can adaptively increase the fraction of H_2 input to preserve the NO_x and NH_3 concentration in the engine exhaust as engine load lowers. Assuming the air-fuel ratio stays relatively constant, NO_x and NH_3 EF can be approximated as a function of indicated specific fuel consumption (ISFC) (see Eq. S1 – S3) which indicates engine efficiency because:

Emission factor of pollutant i (EF_i) can be expressed as the mass of pollutant emitted per unit energy output, which is equivalent to pollutant mass flow rate (ρ_i) per unit power output (P):

$$EF_i = \frac{\rho_i}{P} \text{ (S1)}$$

Power output can be expressed in terms of indicated specific fuel consumption (ISFC, fuel mass flow per unit power output):

$$P = \frac{\rho_f}{ISFC} \text{ (S2)}$$

Where ρ_f is the fuel mass flow rate. This converts the expression of EF_i into:

$$EF_i = \frac{\rho_i}{\rho_f} ISFC = \frac{\left(\frac{\rho_e}{m_e}\right)}{\rho_f} m_i \, C_i \, ISFC \text{ (S3)}$$

Where ρ_e is the exhaust mass flow rate, m_e and m_i are the molar mass of the exhaust mixture and i, respectively, and C_i is the concentration of i in exhaust.

Now we examine equation S3 as a function of engine load. Assuming the air–fuel ratio remains constant, $\frac{\rho_e}{\rho_f}$ = constant by conservation of mass. As most of the combustion mixture consists of inert dinitrogen gas from the air, m_e is also relatively stable. Therefore, if C_i remains relatively constant over a range of load, EF is mostly a function of ISFC. As indicated by Fig. S2, introducing additional H_2 counteracts the trending of decreasing NO_x and increasing NH_3 concentrations as load lowers, leading to relatively stable C_{NH3} and C_{NOx} as load changes. Therefore, we assume that the EF of NH_3–H_2 is solely a function of ISFC.

Since there is no information about the load-dependence of ISFC for NH_3–H_2 engines, we assume that it takes similar shape as that of pure NH_3 engines (Fig. S1d). Though the addition of H_2 increases combustion and thermodynamic efficiency, extra energy would be required to crack more H_2 into NH_3, which lowers the overall efficiency as engine load decreases. Similarly, the N_2O EF and load curve are assumed to be the same between pure NH_3 and NH_3-H_2 engines, due to lack of direct measurements for NH_3-H_2 engines.

Engine emissions are also influenced by engine size and speed, which cannot be directly accounted for in this study due to lack of experimental data. For both pure NH_3 and NH_3–H_2 engines, a 24% of EF penalty is added to ships with lengths under 100m to account for the lower thermodynamic efficiency from smaller engines, which is consistent with Imhoff et al. (2021).

We rely on experimental data from small fast four-stroke engines, which is different from the slow large two-stroke engines that are typical for large commercial vessels (Anantharaman *et al* 2015), since there is no published experimental data for large two-stroke marine engines that uses ammonia as the major energy source. Large two-stroke engines have been shown to have lower unburnt methane (fuel) slip than the smaller four-stroke engines when operating with liquified petroleum gas (Pavlenko *et al* 2020). Thus, our study likely provides an upper bound of NH_3 emissions from ammonia-powered ships.

Effects of turning off PARANOX
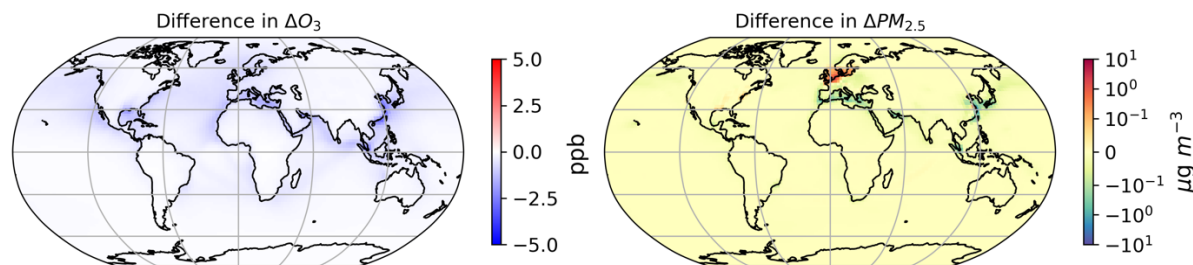
Fig. S3 Differences in modelled responses in annual mean MDA8 O_3 and $PM_{2.5}$ under emissions of $[\text{Pure NH}_3]_{2020}$ when PARANOX is turned off, calculated as $([\text{Pure NH}_3]_{\text{No\_PARANOX}} - \text{Baseline}_{\text{No\_PARANOX}}) - ([\text{Pure NH}_3]_{2020} - \text{Baseline})$

The model result in the main text is performed with PARANOX turned on, which parameterizes the chemical evolution in a typical fossil fuel powered ship plume before it is blended into the background atmosphere. In practice, turning on PARANOX reduces NO_x lifetime by promoting NO_x loss to HNO_3, which is a terminal NO_x sink that deposits rapidly and a $PM_{2.5}$ precursor, affecting both O_3 and $PM_{2.5}$ sensitivity to precursor emissions. Due to distinct chemical composition (e.g. presence of NH_3, absence of SO_x, NMVOC and carbonaceous aerosols), the NO_x lifetime within an ammonia-powered ship plume is highly uncertain.

To briefly explore how might the uncertainty in plume chemistry affect our result, we perform another set of simulations ($[\text{Pure NH}_3]_{2020}$ and baseline) with PARANOX turned off ($[\text{Pure NH}_3]_{\text{NO\_PARANOX}}$ and baseline$_{\text{NO\_PARANOX}}$), which means the ship plume is immediately blended into background atmosphere. While being seemingly less realistic than turning PARANOX on, this configuration can be interpreted as simply assuming a longer NO_x lifetime than that in our standard simulations.

Figure S3 shows the difference in modelled O_3 and $PM_{2.5}$ responses when PARANOX is turned off for $[\text{Pure NH}_3]_{2020}$. PARANOX simulates plume chemistry by converting NO_x emissions into O_3 and HNO_3 before releasing them into model grid cells. When PARANOX is turned off, the NO_x concentration differences between the two scenarios are amplified. Therefore, the modelled O_3 reduction is stronger (more negative) globally by up to 2.8 ppbv, particularly over East Asia, Mediterranean Basin, Red Sea, and Persian Gulf, which significantly impacts ΔM_{O3} (-100,000 versus -73,100 with PARANOX on). Overall, turning off PARANOX does not significantly affect $\Delta M_{PM2.5}$ in global scale (+666,520 versus +668,100 with PARANOX on). However, significant local differences in modelled $PM_{2.5}$ responses of up to 2 µg m^{-3} exist over East Asia and northern Europe, which may be attributable to differences in other NO_x sources near the shore and interactions with concomitant SO_x reductions. The resulting ΔM_{total} with PARANOX off (+566,600) is well within the 95% CI (+448,000; +746,200) of that with PARANOX on. This suggests that the uncertainty in plume chemistry is much more likely to affect modelled O_3 than $PM_{2.5}$ response. While such uncertainty does not affect our main findings (1. Newer engines have lower NO_x emissions, which generally benefits O_3 air quality; 2. unburnt NH_3 emission worsens $PM_{2.5}$ air quality unless it is tightly controlled).

Rough estimate of climate effects from nitrogen deposition

Wolfram *et al* (2022) raise concern about "secondary N_2O emissions" from reactive nitrogen (NH_4^+ +NH_3 + NO_x + Other oxidized nitrogen species derived from NO_x) deposition. This is not a concern NH_3-H_2 engines, since most of the reactive nitrogen from NH_3-H_2 engines is removed by SCR, which converts NO_x and NH_3 into non-reactive forms of nitrogen (N_2 and to lesser extent N_2O). The total reactive nitrogen emissions (and therefore deposition) (3.4 TgN/yr) from NH_3-H_2 engines are lower than that from current fleet (5.3 TgN/yr).

For pure NH_3 engine, most reactive nitrogen emissions are removed through scrubbing, which does not convert reactive nitrogen back to non-reactive forms of nitrogen, leading to large amount of reactive nitrogen entering the Earth Sytstem (60 – 70 TgN/yr). While rigorous evaluations of the impacts of nitrogen deposition on global GHG balance are beyond the scope of this paper, we use scenarios with highest total reactive nitrogen emissions ([Pure NH_3]$_{2020}$) for to briefly discuss about the potential impacts and range of uncertainties of reactive nitrogen deposition on GHG emissions.

Over the ocean, the fraction of ammonium being converted into N_2O vary from 0.01% under typical condition to up to 2% under oxygen depletion (Babbin *et al* 2020). This implies that nitrogen deposition over oxygen minimum zones (OMZ) can have disproportionate impact on N_2O emission. Under the scenario with the largest increases in reactive nitrogen emissions ([Pure NH_3]$_{2020}$), we find a total increase of 5.0 TgN/yr in nitrogen deposition over OMZ (defined as grid cells with O_2 concentration < 20 µM at the most anoxic depth (Paulmier and Ruiz-Pino 2009), with maps of ocean oxygen levels provided by World Ocean Atlas 2018 Garcia *et al* (2019)). If 1% and 0.01% of the depositing reactive nitrogen were converted into N_2O within and outside OMZ, respectively, this would lead to 45.7 Tg $CO_{2,e}$/yr (88% of tailpipe GHG emission from ammonia-powered fleet) increase in GHG emission. Such increases may be offset by increase in global ocean carbon sinks (Jickells *et al* 2017).

We also compare the contemporary effect of nitrogen deposition on GHG balance over land. Yang *et al* (2021) estimate that global nitrogen deposition leads to N_2O emission of 0.89 Tg/yr (= 243 Tg $CO_{2,e}$/yr) over cropland, which is comparable to net climate effect of nitrogen deposition over natural ecosystems (500 Tg $CO_{2,e}$/yr sequestered) (Xiao *et al* 2023). However, another recent study suggests a much smaller increase in forest carbon sequestration (150 Tg CO_2/yr) (Schulte-Uebbing *et al* 2022) due to nitrogen deposition. The net effects of nitrogen deposition on GHG balance over land is therefore highly uncertain. However, it is likely that the net effect is smaller than the reduction in tailpipe GHG emissions from switching to ammonia powered ships (817.2 Tg $CO_{2,e}$/yr). Despite this, with other adverse environmental effects from excessive nitrogen deposition (e.g. eutrophication, soil acidification, biodiversity loss) (Payne *et al* 2017, Baessler *et al* 2019), large amount of reactive nitrogen entering the Earth System is undesirable.

Sensitivity of PM$_{2.5}$ to ammonia emission under presence of sea salt

Under polluted environments, NH$_3$ mostly forms secondary inorganic aerosols with H$_2$SO$_4$ and HNO$_3$, which are the oxidation products of NO$_x$ and SO$_x$:

$$2NH_3 + H_2SO_4 \rightarrow (NH_4)_2SO_4 \text{ (R1)}$$
$$NH_3 + HNO_3 \leftrightarrow NH_4NO_3 \text{ (R2)}$$
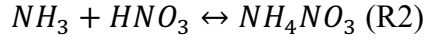
Therefore, if the changes in ammonium aerosols were only caused by interactions with H$_2$SO$_4$ and HNO$_3$, the changes in ammonium, sulphate and nitrate aerosols should follow the stoichiometry prescribed by R1 and R2. In contrast, if the changes in ammonium, sulphate and nitrate aerosols were not stoichiometric, that could indicate alternative aerosol formation pathways that alters the sensitivity of secondary inorganic PM$_{2.5}$ level to precursor emissions, which is highly possible over the ocean due to presence of ion-rich sea spray aerosols.

To examine the potential impacts of such alternative aerosol formation pathways, we calculate the deviation of changes in ammonium PM$_{2.5}$ mass from the stoichiometric conditions of the NH$_3$–H$_2$SO$_4$–HNO$_3$ system (ΔM^*_{NH4}) from [NH$_3$–H$_2$]$_{2020}$ run, which is shown in Figure S4:

$$\Delta M^*_{NH_4} = 1.1\rho m_{NH_4}\left(\Delta C_{NH_4} - 2\Delta C_{SO_4} - \Delta C_{NO_3}\right) \text{ (S4)}$$

Where ρ is the molar density of air, m$_{NH4}$ is molar mass of NH$_4$, ΔC_i are the concentration changes of the corresponding secondary inorganic aerosol species. The factor 1.1 is included to match the standard conditions of PM$_{2.5}$ measurements used in the main manuscript.
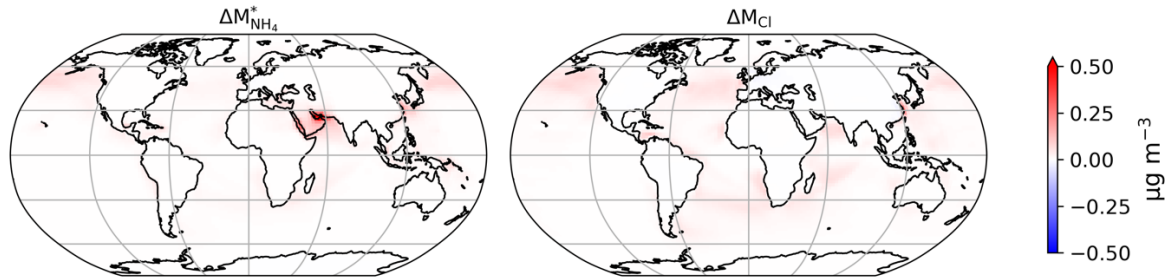
Fig. S4. Deviation of changes in ammonium PM$_{2.5}$ mass from stoichiometric conditions (ΔM^*_{NH4}) as calculated by Equation S4, and changes in PM$_{2.5}$ mass from sea salt chloride (ΔM_{Cl})

We find that ΔM^*_{NH4} is always positive, with largest value of 0.7 μg m^{-3} around the Arabian Peninsula. While studying the detailed chemical interactions between NH$_3$ and other atmospheric acids and ions is beyond the scope of this paper, one possible explanation of positive ΔM^*_{NH4} is aerosol formation with other anions within sea salt aerosols (e.g. chloride as shown in Figure S4). Also, fine sea spray aerosols are inherently acidic (Angle *et al* 2021), which could react with NH$_3$ independently. This shows the existence of extra sensitivity of PM$_{2.5}$ to NH$_3$ in marine environment that is independent to SO$_x$ and NO$_x$ emissions. Thus, controlling coastal and marine NO$_x$ and SO$_x$ alone could not eliminate the sensitivity of PM$_{2.5}$ to NH$_3$ emissions.

Excessive Water Vapor generated from Ammonia Combustion

The mass of water vapor generated per unit energy released from complete combustion of fuel i ($m_{w,i}$) can be calculated as:

$$m_{w,i} = \frac{1}{LHV_i}\left(\frac{M_w}{M_i}\right)\lambda_{w_i} \text{ (S4)}$$

where LHV_i = the Lower Heating Value (LHV) of fuel i, M_w = molar mass of water, M_i = molar mass of fuel i, $\lambda_{w,i}$ = moles of water formed per moles of fuel i under complete combustion. Using lower heating values at 25 °C of diesel (43.4 MJ/kg) (Linstrom 1997) and ammonia (18.8 MJ/kg) (Valera-Medina et al 2018), and taking the average chemical formula of diesel to be $C_{12}H_{23}$ (Date and Date 2011), $m_{w,diesel}$ = 28.6 g/MJ and $m_{w,ammonia}$ = 84.5 g/MJ. This implies for a given amount of energy released, complete combustion of ammonia generates two times more water vapor than diesel.

Another equation (S5) can be derived from equation S4 to explain the difference between $m_{w,diesel}$ and $m_{w,ammonia}$:

$$\frac{m_{w,ammonia}}{m_{w,diesel}} = \frac{LHV_{diesel}}{LHV_{ammonia}}\left(\frac{M_{ammonia}}{M_{diesel}}\frac{\lambda_{w,diesel}}{\lambda_{w,ammonia}}\right) = \frac{LHV_{diesel}}{LHV_{ammonia}}R \text{ (S5)}$$

R = 1.27, while $\frac{LHV_{diesel}}{LHV_{ammonmoia}}$ = 2.31. Therefore, the excessive water vapor generated from ammonia combustion is mainly attributable to its low LHV.

Reference

Anantharaman M, Garaniya V, Khan F and Lewarn B 2015 Marine engines and their impact on the economy, technical efficiency and environment *Marine Engineering* **50** 360–7

Angle K J, Crocker D R, Simpson R M C, Mayer K J, Garofalo L A, Moore A N, Mora Garcia S L, Or V W, Srinivasan S, Farhan M, Sauer J S, Lee C, Pothier M A, Farmer D K, Martz T R, Bertram T H, Cappa C D, Prather K A and Grassian V H 2021 Acidity across the interface from the ocean surface to sea spray aerosol *Proceedings of the National Academy of Sciences* **118** e2018397118

Babbin A R, Boles E L, Mühle J and Weiss R F 2020 On the natural spatio-temporal heterogeneity of South Pacific nitrous oxide *Nature Communications* **11**

Baessler C, Bonn A, Klotz S, Schröter M and Seppelt R 2019 *Atlas of Ecosystem Services: Drivers, Risks, and Societal Responses* (Cham: Springer International Publishing : Imprint: Springer)

Date A W and Date A W 2011 *Analytic combustion: with thermodynamics, chemical kinetics, and mass transfer* (Cambridge: Cambridge University Press)

Garcia H E, Weathers K W, Paver C R, Smolyar I, Boyer T P, Locarnini M M, Zweng M M, Mishonov A V, Baranova O K and Seidov D 2019 World Ocean Atlas 2018, Volume 3: Dissolved Oxygen, Apparent Oxygen Utilization, and Dissolved Oxygen Saturation.

Imhoff T B, Gkantonas S and Mastorakos E 2021 Analysing the performance of ammonia powertrains in the marine environment *Energies* **14**

Jickells T D, Buitenhuis E, Altieri K, Baker A R, Capone D, Duce R A, Dentener F, Fennel K, Kanakidou M, LaRoche J, Lee K, Liss P, Middelburg J J, Moore J K, Okin G, Oschlies A, Sarin M, Seitzinger S, Sharples J, Singh A, Suntharalingam P, Uematsu M and Zamora L M 2017 A reevaluation of the magnitude and impacts of anthropogenic atmospheric nitrogen inputs on the ocean *Global Biogeochemical Cycles* **31**

Lhuillier C, Brequigny P, Contino F and Mounaïm-Rousselle C 2020 Experimental study on ammonia/hydrogen/air combustion in spark ignition engine conditions *Fuel* **269**

Linstrom P 1997 NIST Chemistry WebBook, NIST Standard Reference Database 69 Online: http://webbook.nist.gov/chemistry/

Mercier A, Mounaïm-Rousselle C, Brequigny P, Bouriot J and Dumand C 2022 Improvement of SI engine combustion with ammonia as fuel: Effect of ammonia dissociation prior to combustion *Fuel Communications* **11**

Mounaïm-Rousselle C, Bréquigny P, Dumand C and Houillé S 2021 Operating limits for ammonia fuel spark-ignition engine *Energies* **14**

Mounaïm-Rousselle C, Mercier A, Brequigny P, Dumand C, Bouriot J and Houillé S 2022
Performance of ammonia fuel in a spark assisted compression Ignition engine
International Journal of Engine Research **23**

Paulmier A and Ruiz-Pino D 2009 Oxygen minimum zones (OMZs) in the modern ocean
Progress in Oceanography **80** 113–28

Pavlenko N, Comer B, Zhou Y, Clark N and Rutherford D 2020 *The climate implications of
using LNG as a marine fuel* (Stockholm, Sweden: Swedish Environmental Protection
Agency)

Payne V H, Neu J L and Worden H M 2017 Commentary on "O3 variability in the troposphere as
observed by IASI over 2008–2016: Contribution of atmospheric chemistry and
dynamics" by wespes et al. *Journal of Geophysical Research* **122** 6130–4

Schulte-Uebbing L F, Ros G H and de Vries W 2022 Experimental evidence shows minor
contribution of nitrogen deposition to global forest carbon sequestration *Global Change
Biology* **28**

Valera-Medina A, Xiao H, Owen-Jones M, David W I F and Bowen P J 2018 Ammonia for
power *Progress in Energy and Combustion Science* **69** 63–102

Wolfram P, Kyle P, Zhang X, Gkantonas S and Smith S 2022 Using ammonia as a shipping fuel
could disturb the nitrogen cycle *Nature Energy* **7** 1112–4

Xiao S, Wang C, Yu K, Liu G, Wu S, Wang J, Niu S, Zou J and Liu S 2023 Enhanced CO2
uptake is marginally offset by altered fluxes of non-CO2 greenhouse gases in global
forests and grasslands under N deposition *Global Change Biology*

Yang Y, Liu L, Zhang F, Zhang X, Xu W, Liu X, Wang Z and Xie Y 2021 Soil Nitrous Oxide
Emissions by Atmospheric Nitrogen Deposition over Global Agricultural Systems
Environmental Science and Technology **55**